



CHORUS

This is the accepted manuscript made available via CHORUS. The article has been published as:

Negative absolute conductivity in photoexcited metals

Giuliano Chiriacò, Andrew J. Millis, and Igor L. Aleiner

Phys. Rev. B **101**, 041105 — Published 13 January 2020

DOI: [10.1103/PhysRevB.101.041105](https://doi.org/10.1103/PhysRevB.101.041105)

Negative absolute conductivity in photoexcited metals

Giuliano Chiriacò,¹ Andrew J. Millis,^{1,2} and Igor L. Aleiner¹

¹*Department of Physics, Columbia University, New York, NY 10027*

²*Center for Computational Quantum Physics, The Flatiron Institute, New York, NY 10010*

(Dated: December 17, 2019)

We show that in a model of a metal photoexcited by a transient pump pulse resonant with a phonon mode, the absolute dc conductivity may become negative, depending on the interplay between the electronic structure, the phonon frequency and the pump intensity. The analysis includes the effects of inelastic scattering and thermal relaxation. Results for the time evolution of the negative conductivity state are presented; the associated non-equilibrium physics may persist for long times after the pulse. Our findings provide a theoretical justification for previously proposed phenomenology and indicate new routes to the generation and exploration of intrinsically non-equilibrium states.

The dc electrical conductivity σ (ratio of current j to applied field E) is a fundamental property of materials. In thermal equilibrium the linear response conductivity is non negative because an applied electric field creates entropy via Joule heating σE^2 and the entropy production rate must be non-negative. Beyond the linear response regime new effects may occur. For example negative *differential* conductivity $\sigma_{\text{diff}} \equiv dj/dE|_{E \neq 0} < 0$ has been extensively studied [1–3] and is typically related to runaway heating at current driven metal-insulator transitions. This paper is concerned with the less commonly realized situation of negative *absolute* conductivity (NAC), $\sigma \equiv j/E < 0$. A negative absolute conductivity state is possible away from thermal equilibrium because the entropy decrease implied by the σE^2 term can be compensated by other sources of entropy production, and would lead to remarkable phenomenological consequences including novel response properties [4–6] spontaneously generated internal electric fields [7], and new collective modes [8] that might be relevant to recent experimental studies of the transient optical properties in photoexcited K_3C_{60} [9]. It is therefore important to understand the circumstances under which a negative absolute conductivity can occur.

Insight into the origin of the NAC state may be obtained from the expression $\sigma = \int d\varepsilon \tilde{\sigma}(\varepsilon)(-\partial_\varepsilon f)$, with $\tilde{\sigma}(\varepsilon) = e^2 \langle v^2(\varepsilon) \rangle D(\varepsilon) \tau_{\text{tr}}(\varepsilon)$, where e is the electron charge, $\langle v^2 \rangle$ is a suitably averaged electron velocity, D is the density of states, τ_{tr} is the transport scattering time and f is the electron distribution function. $\tilde{\sigma}$ is always positive and in equilibrium $-\partial_\varepsilon f > 0$. However, out of equilibrium $-\partial_\varepsilon f$ may become negative in some energy regions; we refer to this situation as a local (in energy) population inversion. If the energy regions where $-\partial_\varepsilon f < 0$ coincide with maxima of $\tilde{\sigma}$, then the total conductivity may become negative. Regions of $-\partial_\varepsilon f < 0$ were shown to occur and to lead to negative absolute conductivity in the two dimensional electron gas subject to a perpendicular magnetic field and to a steady state microwave radiation [10–12], **and more recently in a steadily photoexcited correlated insulator** [13]; for example, in the first system the peaked energy structure in $\tilde{\sigma}$ was caused

by Landau level quantization and the regions of local inversion were produced by the drive at a frequency that matched the Landau level spacing.

In this paper we show that a local population inversion can occur in a system of electrons coupled to strongly pumped phonons, and that this inversion can lead to a NAC state, even when the pumping is not continuous; indeed, the effect can be induced by transiently pumped phonons and can persist for long times after the pump is removed. We show how the NAC state depends on the intensity of the driving pump and that the effect is maximized if the phonon frequency is approximately commensurate with the distance from Fermi energy to the band edges; we provide information on which forms of the electron and phonon density of states create the most likely conditions for the effect to occur. We estimate the coupling constant from the phenomenological theory of Ref. [8] and explicate the effects of internal electric fields and energy relaxation mechanisms.

The model - We study a metallic system, initially in equilibrium at temperature T , characterized by a dispersionless phonon mode with energy ω_p ; a weak dispersion is important, as discussed below. We assume (as in the usual theory of electron-phonon coupling) that the electrons and phonons can be described in a quasiparticle picture. Introducing the operators $c_{\mathbf{k}}$, $c_{\mathbf{k}}^\dagger$ and $a_{\mathbf{q}}$, $a_{\mathbf{q}}^\dagger$ for electron and phonons respectively, the Hamiltonian can be written as

$$H = \sum_{\mathbf{k}} \epsilon_{\mathbf{k}} c_{\mathbf{k}}^\dagger c_{\mathbf{k}} + \sum_{\mathbf{q}} \omega_p a_{\mathbf{q}}^\dagger a_{\mathbf{q}} + H_{\text{el-ph}}; \quad (1)$$

where $H_{\text{el-ph}} = \sum_{\mathbf{k}, \mathbf{q}} M_{\mathbf{q}} (a_{-\mathbf{q}}^\dagger + a_{\mathbf{q}}) c_{\mathbf{k}}^\dagger c_{\mathbf{k}-\mathbf{q}}$, with $M_{\mathbf{q}}$ the electron-phonon interaction matrix element, and $\epsilon_{\mathbf{k}}$ is the electron energy dispersion.

We assume that the system is photoexcited by radiation that induces a highly non-equilibrium state of the phonons and we assume that the phonon coherence and momentum relax very quickly, so we may characterize the non-equilibrium phonon population by a diagonal, momentum independent distribution function $\langle a_{\mathbf{q}}^\dagger a_{\mathbf{q}} \rangle = \zeta + b$, which is the sum of the thermal distribution $b = (e^{\omega_p/T} - 1)^{-1}$ and a non equilibrium compo-

ment ζ . Because of the momentum independence of ζ we can average all the relevant electronic properties over \mathbf{k} and characterize the system by ζ , the electron distribution $f(\varepsilon)$, the density of states $D(\varepsilon)$, the average velocity squared $v^2(\varepsilon)$ and the transport scattering time τ_{tr} [14].

We study the non-equilibrium dynamics of the system using the Keldysh formalism within Migdal-Eliashberg theory; the supplemental material provides a detailed treatment. We find as in equilibrium that the electron density of states (retarded part of the Green function) and the phonon frequency are only slightly renormalized by the non-equilibrium drive [15]. We therefore focus on the electron distribution function f and on the non-equilibrium part of the phonon population ζ , which are the solution of two coupled kinetic equations:

$$\partial_t f + \text{St}_E\{f\} = \text{St}_{in}\{f\} + \text{St}_{el}\{f, \zeta\}; \quad (2)$$

$$\partial_t \zeta = \text{St}_{ph}\{f, \zeta\} + I_p(t) - \zeta/\tau_{ph}, \quad (3)$$

where St_E is the effect of the dc electric field E , St_{in} is the inelastic scattering term, St_{el} and St_{ph} are the contributions of the electron-phonon interaction to the collision integrals of f and of ζ respectively, $I_p(t)$ a phonon source term arising from the pump and the initial decoherence processes, and τ_{ph} is the decay time for ζ , due to inelastic scattering with other phonons [15]. **Notice that in general the pump pulse also affects the electrons, but it has essentially the same effects a phonons, since it drives the same electronic transitions; for simplicity we neglect this effect, since it would not affect the steady state electron distribution and would just accelerate the initial evolution of the electrons in the transient regime.**

Neglecting for simplicity the \mathbf{q} dependence of $M_{\mathbf{q}}$, we evaluate the collision integral for electrons and phonons

$$\text{St}_{el} = \frac{\Gamma_{eph}}{D_0} \left(D_{\varepsilon-\omega_p} [(\zeta + b)(f_{\varepsilon-\omega_p} - f_\varepsilon) - f_\varepsilon(1 - f_{\varepsilon-\omega_p})] + D_{\varepsilon+\omega_p} [(\zeta + b)(f_{\varepsilon+\omega_p} - f_\varepsilon) + f_{\varepsilon+\omega_p}(1 - f_\varepsilon)] \right) \quad (4)$$

$$\text{St}_{ph} = \frac{\Gamma_{eph}}{D_0} \int D(\varepsilon) D(\varepsilon + \omega_p) \left[f(\varepsilon + \omega_p)(1 - f(\varepsilon)) + (\zeta + b)(f(\varepsilon + \omega_p) - f(\varepsilon)) \right] d\varepsilon, \quad (5)$$

where $\Gamma_{eph} \equiv 2\pi|M|^2 D_0$ is the electron-phonon scattering rate and D_0 is the average electron density of states. Equation (4) has an evident periodicity in energy, which at $\zeta \gg 1$ induces a periodic distribution $f(\varepsilon)$ with period ω_p ; for such distribution, both St_{el} and St_{ph} approximately vanish.

We model the inelastic scattering as arising from the coupling to a thermal bath at temperature T ; if the energy is exchanged in small amounts, the scattering is an energy diffusion process with effective rate Γ_{in} :

$$\text{St}_{in} = \frac{\Gamma_{in}}{D_F} \frac{1}{D(\varepsilon)} \partial_\varepsilon \left[D^2(\varepsilon) [T \partial_\varepsilon f + f(1 - f)] \right], \quad (6)$$

St_{in} makes the electrons relax to a Fermi-Dirac distribution with temperature T .

It will also be important to consider an applied dc electric field. As shown in the supplemental material, this causes a diffusion in energy space

$$\text{St}_E = -\frac{E^2}{3} \frac{1}{D(\varepsilon)} \partial_\varepsilon [\tilde{\sigma}(\varepsilon) \partial_\varepsilon f(\varepsilon)], \quad (7)$$

where $\tilde{\sigma}(\varepsilon) = e^2 v^2(\varepsilon) D(\varepsilon) \tau_{tr}$. We see from Eq. (7) that the electric field smooths out the steepest regions in f , creating a pseudo-thermal distribution [16, 17] with effective temperature $T_{\text{eff}} \sim T + e^2 E^2 v_F^2 \tau_{tr} / \Gamma_{in}$, where v_F is the Fermi velocity.

Equations (2)-(7) are a complete system that can be solved for $f(\varepsilon, t)$ and $\zeta(t)$ given a source term $I_p(t)$. We consider two limiting cases: *i*) a steady state drive; *ii*) a short pump pulse occurring over a time τ_{pulse} much smaller than the relaxation time of the transient state.

Population inversion for steady state drive - In equilibrium ($\zeta = 0$, $E = 0$) Eq. (2) is solved by the thermal Fermi-Dirac distribution $f_T(\varepsilon)$. To gain a first understanding of the non-equilibrium physics, we neglect inelastic scattering of electrons ($\text{St}_{in} \rightarrow 0$), electric field and phonon dynamics; we assume the system to be in equilibrium at temperature T for $t < 0$ and that at $t = 0$ the phonon distribution is instantaneously switched to a state with $\zeta > 0$. We then solve Eq. (2) for fixed ζ and consider the long time limit.

The dispersionless phonon approximation means that an electronic state at energy ε is coupled to the discrete set of states at energy $\varepsilon + j\omega_p$, with j an integer such that $\varepsilon + j\omega_p$ is within the band of allowed states. Since the scattering conserves particles number, $\sum_j D(\varepsilon + j\omega_p) f(\varepsilon + j\omega_p)$ is time independent and thus equal to the initial value $\sum_j D(\varepsilon + j\omega_p) f_T(\varepsilon + j\omega_p)$. In the large ζ limit, $f(\varepsilon)$ must be periodic in ε so that $\text{St}_{el} = 0$, i.e. $f(\varepsilon + \omega_p) = f(\varepsilon)$, implying

$$f(\varepsilon) = \frac{\sum_j D(\varepsilon + j\omega_p) f_T(\varepsilon + j\omega_p)}{\sum_j D(\varepsilon + j\omega_p)} \quad (8)$$

The particular shape of $f(\varepsilon)$ depends on the DoS and on ω_p . In the $T \rightarrow 0$ limit, the ε structure of f is controlled by the energy dependence of D in the range between the chemical potential μ and the lower band edge, except for down steps at $\varepsilon + j\omega_p = \mu$ or steps of either sign when $\varepsilon + j\omega_p$ matches a singularity in the DoS. Since f is periodic, the down steps must be matched by an average increase of f .

Results of a numerical solution of Eq. (2) are shown in Fig. 1 for a trial density of states. Here D is an increasing function of ε between the lower band edge and μ and we see that f is characterized by regions of smooth increase separated by downward jumps at $\varepsilon = \mu - j\omega_p$; the distribution arising from an alternative DoS (with singularities at the band edges) is shown in the supplemental. Panels (a) and (b) of Fig.1 show the $\text{St}_{in} \rightarrow 0$ limit at different doping levels. Panels (c) and (d) show the effects of including the inelastic scattering (c) and a

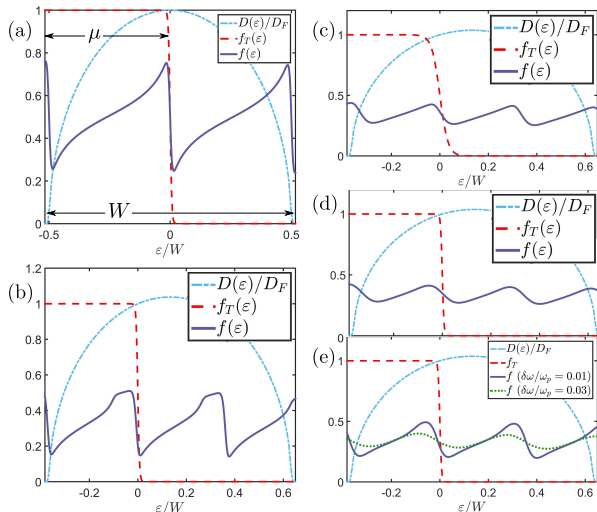


FIG. 1. Non-equilibrium steady state electron distribution f (blue solid lines), obtained from solution of Eq. (2) for a steady state phonon population $\zeta = 20$, trial DoS $D(\varepsilon)$ (cyan dashed-dotted lines) normalized to the Fermi DoS D_F , initial distribution given by a Fermi-Dirac f_T (red dashed) at chemical potential μ and temperature $T/W = 0.003$ (a), (b), (d), (e) and $T/W = 0.02$ (c). The phonon frequency is $\omega_p/W = 0.5$ (a) and $\omega_p/W = 0.36$ (b)-(e). Panel (c) includes a stronger inelastic scattering $St_{in}/St_{el} \sim 0.05$; in panel (d) we use the parameters of (b) but with field $eEv_F\sqrt{\tau_{tr}/\Gamma_{in}}\omega_p = 0.4$; in panel (e) we use the parameters of (b) and a dispersive phonon with typical width $\delta\omega/\omega_p = 0.01, 0.03$.

dc electric field (d); both these terms lead to diffusion in energy space, smoothing out f similarly to raising T .

We also analyze the consequences of a dispersive phonon frequency with typical width $\delta\omega$. This leads to an additional diffusion-like term in St_{el} [15], which renormalizes the temperature $T \rightarrow T_{eff} = T + \zeta\delta\omega$ and smooths the local population inversion when $T_{eff} \approx \omega_p$, i.e. $\delta\omega/\omega_p \gtrsim 1/\zeta$ (Fig. 1e). In the rest of the paper, we neglect the effects of a dispersive band, but allow for a small inelastic scattering and for non zero dc fields.

Steady state conductivity - An analysis of the Keldysh equations yields for the conductivity [15]

$$\sigma = \int \tilde{\sigma}(\varepsilon) (-\partial f / \partial \varepsilon) d\varepsilon. \quad (9)$$

The sign of σ depends on how regions with large and small values of $\tilde{\sigma}(\varepsilon)$ are matched to the regions of normal and inverted population. An expression for σ can be derived by approximating $-\partial_\varepsilon f$ as the sum of delta functions at $\varepsilon = \mu + j\omega_p$ and smooth terms; for the DoS of Fig. 1, $-\partial_\varepsilon f \sim -1/\omega_p$ and we obtain

$$\sigma \sim \sum_j \tilde{\sigma}(\mu + j\omega_p) - \frac{1}{\omega_p} \int d\varepsilon \tilde{\sigma}(\varepsilon) \quad (10)$$

From Eq. (10) we see that when ω_p is such that $\mu + j\omega_p$ corresponds to a band edge (where $\tilde{\sigma}(\varepsilon)$ is small) for some

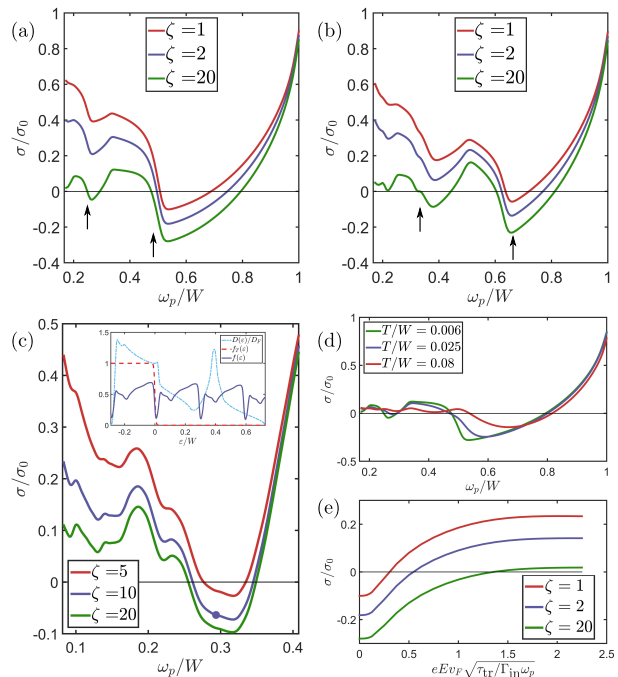


FIG. 2. (a)-(b) Plot of normalized conductivity σ/σ_0 (where $\sigma_0 \equiv v_F^2\tau_{tr}D_F$) as function of ω_p for three values of ζ at $T/W = 0.003$, $E = 0$ for the DoS of Fig.1; the filling is $1/2$ ($\mu = 0$) in (a) and $1/3$ ($\mu \approx -W/6$) in (b); the arrows indicate the values of ω_p corresponding to the commensurability criteria, i.e. $\omega_p/W = 1/4, 1/2$ in (a) and $\omega_p/W = 1/3, 2/3$ in (b). (c) Plot of σ/σ_0 for a different DoS (modeling p -like electrons in cubic symmetry) as function of ω_p at $T/W = 0.003$ and half filling; the inset shows the corresponding DoS D and distribution f for the frequency ω_p marked with a dot on the graph. (d)-(e) Plot of σ/σ_0 at half filling as function of ω_p at $\zeta = 20$ and $E = 0$ for three different temperatures (d) and as function of the normalized electric field E at $\omega_p/W = 0.53$ and $T/W = 0.003$ (e). Calculations were performed for $\Gamma_{in} \ll \Gamma_{eph}$ assuming constant $v^2\tau_{tr}$ and the system was evolved for a time $10\Gamma_{eph}^{-1}$.

j , the positive term in σ may be outweighed by the negative contribution of the integral. This is most likely to happen when ω_p is commensurate with the distance of either of the band edge energies from the chemical potential, as confirmed by numerical calculations of $\sigma(\omega_p)$ performed in the limit of constant $v^2\tau_{tr}$ [18], see Fig. 2; indeed the effect is enhanced when the chemical potential is such that ω_p is commensurate with both band edges energies at the same time, see Fig. 1a and 2a ($1/2$ -filling). A similar criterion holds for more complicated density of states, such as a double peaked structure modeling p -like electrons in a cubic lattice; in this case $\sigma(\omega_p) < 0$ also when ω_p is commensurate with the distance from Fermi level to the minimum of $D(\varepsilon)$ (Fig. 2c).

Figure 2 shows that when plotted as function of the phonon frequency, the conductivity minima generally occur at frequencies slightly bigger than the values of ω_p satisfying the commensurability criteria. The dependence on ζ (pump strength) saturates rapidly as ζ is increased above 1.

From these results we conclude that a system can exhibit a negative conductivity when: (i) the DoS is **on average** an increasing function of ε in the region of equilibrium occupied states. (ii) The pump is strong enough to induce a sizeable population inversion of the electrons. (iii) The phonon frequency ω_p is roughly commensurate with a relevant energy scale in the density of states, e.g. the distance from the Fermi level to the edges of the band or to a minimum of $\tilde{\sigma}$.

In Fig. 2d and 2e we report the dependence of $\sigma(\omega_p)$ on temperature and dc field, for the trial DoS of Fig. 1. We find that the negative conductivity is suppressed at high temperatures (Fig. 2d) and by an electric field (Fig. 2e). In particular, Joule heating dominates the entropy production at high fields, so $\sigma(E)$ must become positive as E increases: thus if $\sigma(E=0) < 0$, there exists a field E^* for which the conductivity vanishes, $\sigma(E^*) = 0$. The value of E^* is set by the scattering length $v_F\sqrt{\tau_{tr}/\Gamma_{in}}$ and depends on the details of the system. Roughly, $\sigma > 0$ when either St_{in} or St_E are large enough to smooth out the local population inversion, i.e. when the effective temperature gets of the order of ω_p , or $E^* \sim \sqrt{\omega_p\Gamma_{in}/\tau_{tr}}/e v_F$. This rough estimate agrees with Fig. 2e.

Short photoexcitation pulse - We now consider a short pump pulse and study the subsequent evolution of f and ζ . We show that the system may develop a transient NAC state that persists after the drive is switched off. We describe the pump pulse with a characteristic strength ζ_0 [19] and a duration τ_{pulse} ; we consider a pulse much shorter than the relaxation time, so that the time scales involved are well separated. We also assume that the inelastic scattering is small $St_{el} \gg St_{in}$ (or $\Gamma_{in} \ll \Gamma_{eph}$).

We solve numerically Eqs. (2)-(7) for the trial DoS of Fig. 1 and plot the behavior of σ and ζ as function of time for $\Gamma_{eph}\tau_{ph} = 5$ in Fig. 3a. After the pump is switched on, $\zeta(t)$ grows rapidly ($t \sim \tau_{pulse}$) and the system develops a negative σ ($t \sim \Gamma_{eph}^{-1}$); ζ then relaxes back to equilibrium ($t \sim \tau_{ph}$) and σ returns positive. **The NAC state occurs if it can develop before the system relaxes, i.e. if $\Gamma_{eph}^{-1} \ll \tau_{ph}$; its lifetime is $\sim \tau_{ph} \gg \tau_{pulse}$, showing the persistence of the NAC state long after the driving pulse is removed, and exhibits a slight decrease at higher T or lower ζ_0 , as expected.**

We can see from Eq. (3) why the relaxation timescale is $\sim \tau_{ph}$ and not Γ_{eph}^{-1} . This occurs because, after an initial energy transfer from the phonon mode to the electrons, the system attains an approximate steady state in which there is no further energy transfer between electrons and phonon, **because f is ω_p -periodic leading to $St_{el} \approx 0$ and $St_{ph} \approx 0$** . In this situation the phonon mode can relax either through the other phonons (scale $\sim \tau_{ph}$) or indirectly because of the inelastic scattering of the electrons (scale $\sim \Gamma_{in}^{-1}$); in our framework, both these timescales are longer than Γ_{eph}^{-1} , leading to a rather long lived non-equilibrium state.

The results in Fig. 3a neglect the instability associated to a negative conductivity: for $\sigma < 0$ any charge fluctuation grows exponentially with a characteristic time

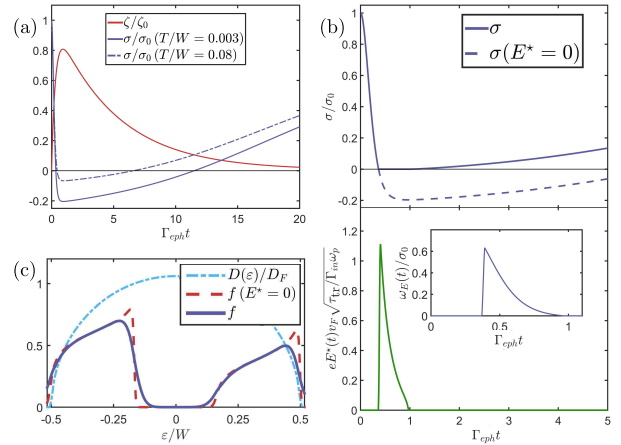


FIG. 3. (a) Plot of σ/σ_0 (blue) and ζ/ζ_0 (red) as function of time $\Gamma_{eph}t$ at 1/3-filling, $\zeta_0 = 10$, $\omega_p/W = 2/3$ eV, $T/W = 0.003$ (solid) and $T/W = 0.08$ (dashed) for $\Gamma_{eph}\tau_{pulse} = 0.3$ and $\Gamma_{eph}\tau_{ph} = 5$. (b) Upper panel: plot as function of time $\Gamma_{eph}t$ of σ/σ_0 (blue) for the two scenarios with (solid) and without (dashed) considering the $\sigma < 0$ instability; bottom panel: plot as function of time of $E^*(t)$, for the same parameters as (a); the inset shows the parameter $\omega_E(t)$ normalized to σ_0 . (c) Plot of $D(\varepsilon)$ and of the distribution f at $\Gamma_{eph}t = 5$; the red dashed curve refers to the scenario with no $\sigma < 0$ instability ($E^* = 0$), while the solid blue curve takes the instability into account. We used the trial DoS from Fig. 1 and modeled the pulse as a decaying exponential $I_p(t) = \zeta_0\tau_{pulse}^{-1}e^{-t/\tau_{pulse}}$ for $t > 0$.

$\tau_M^{-1} = 4\pi|\sigma|$ [7, 8]; for a typical metal $\tau_M \lesssim 1$ fs. This time is much smaller than the typical values of τ_{pulse} , so we can assume that the system instantaneously tunes itself to a state with a spontaneous polarization $|\vec{E}| = E^*$ such that $\sigma(E^*) = 0$. We take into account the instability by including the contribution of Eq. (7) to the collision integral, with $E^*(t)$ chosen so that if the solution of Eq. (2) predicts $\sigma(t) < 0$, $\sigma(t, E^*(t)) = 0$.

In Fig. 3b we plot $\sigma(t)$ and $E^*(t)$; the value of the field is comparable with the steady state values found previously in Fig. 2e. The field grows very rapidly in a short time $\sim \tau_M$ and then decays following the relaxation of $\zeta(t)$; notice that $E^*(t)$ goes to zero in a finite time and with a non zero derivative, because the conductivity turns back positive when $\zeta(t)$ decays below a certain threshold. This internal field does not affect the decay of ζ , but smooths out the regions of inverted population in f , as observed in Fig. 3c: the non-equilibrium distributions at equal times are compared for the cases $E^* = 0$ and $E^* \neq 0$ finding a weakening of the local population inversions. This leads to a faster relaxation towards equilibrium, so that the zero conductivity state has a shorter lifetime than the NAC state (Fig. 3b).

Finally to make a connection to the phenomenological analysis of Ref. [8], we estimate the parameter ω_E , i.e. the sensitivity of entropy production to perturbations of the total energy. Notice that in Ref. [8] the total energy of the system is conserved after the pulse, while in this paper we allow for energy relaxation through St_{in} and τ_{ph} . Therefore, although the connection would be techni-

cally imprecise, we can still estimate ω_E as the derivative of the Joule heating contribution to entropy production with respect to fluctuations of the electric field energy: $\omega_E \sim \partial\sigma/\partial E^2|_{E^*} (E^*)^2$; $\omega_E(t)$ depends on time and goes to zero as $E^*(t) \rightarrow 0$, see inset in Fig. 3b.

Conclusions - We have studied a minimal microscopic model for the transient conductivity of a photoexcited metal, in which the pump drives a strong non-equilibrium phonon distribution, that may induce an inverted electron population.

We found the conditions for the occurrence of the population inversion and studied the dynamics of this transient state, considering the relaxation of phonons and electrons. We found that for certain pump energies (dependent on the band structure and the doping level), the photoexcited system develops an absolute negative conductivity state. **Ideal systems that may exhibit such state**

have electron-phonon coupling strong enough so that the related scattering time is faster than the relaxation time of the system; they also have a commensurate ratio between phonon frequency and bandwidth, which is easily achieved in the case of narrow bandwidth and/or high frequency phonons. The negative conductivity state is unstable and evolves into a state with zero conductivity and a spontaneous electric polarization. We showed that this transient state persists even after the pump has been removed and that the spontaneous electric field does not destroy immediately the zero conductivity state, but rather reduces its lifetime.

Acknowledgements - Support was provided by the Basic Energy Sciences Division of the Office of Science of the United States Department of Energy under Grant No. DE-SC0018218 (A.M. and G.C.) and by the Simons Foundation (I.A.).

-
- [1] A. L. Zakharov, Zh. Eksp. Teor. Fiz. **38**, 665 (1960); Sov. Phys. JETP **11**, 478 (1960).
- [2] A. F. Volkov and S. M. Kogan, Sov. Phys. Usp. **11**, 881 (1969).
- [3] B. K. Ridley, Proc. Phys. Soc. **82**, 954 (1963); **86**, 637 (1965).
- [4] R. G. Mani, J. H. Smet, K. von Klitzing, V. Narayana-murti, W. B. Johnson, and V. Umansky, Nature **420**, 646 (2002).
- [5] M. A. Zudov, R. R. Du, L. N. Pfeiffer, and K. W. West, Phys. Rev. Lett. **90**, 046807 (2003).
- [6] V. I. Ryzhii, Fiz. Tverd. Tela **11**, 2577 (1970), [Sov. Phys. Solid State, **11**, 2078 (1970)]; V. I. Ryzhii, R. A. Suris, and B. S. Shchamkhalova, Fiz. Tekh. Poluprovodn **20**, 2078 (1986), [Sov. Phys. Semiconductors, **20**, 1289 (1986)].
- [7] A. V. Andreev, I. L. Aleiner, and A. J. Millis, Phys. Rev. Lett. **91**, 056803 (2003).
- [8] G. Chiriacò, A. J. Millis, and I. L. Aleiner, Phys. Rev. B **98**, 220510(R) (2018).
- [9] M. Mitranò, A. Cantaluppi, D. Nicoletti, S. Kaiser, A. Perucchi, S. Lupi, P. Di Pietro, D. Pontiroli, M. Riccò, S. R. Clark, D. Jaksch, and A. Cavalleri, Nature **530**, 461 (2016).
- [10] A. C. Durst, S. Sachdev, N. Read, and S. M. Girvin, Phys. Rev. Lett. **91**, 086803 (2003).
- [11] M. I. D'yakonov, Pis'ma Zh. Eksp. Teor. Fiz. **39**, 158 (1984), [JETP Lett., **39**, 185 (1984)]; M. I. D'yakonov and A. S. Furman, Zh. Eksp. Teor. Fiz. **87**, 2063 (1984), [Sov. Phys. JETP, **60**, 1191 (1984)].
- [12] I. A. Dmitriev, M. G. Vavilov, I. L. Aleiner, A. D. Mirlin, and D. G. Polyakov, Phys. Rev. B **71**, 115316 (2005).
- [13] N. Tsuji, T. Oka, and H. Aoki, Phys. Rev. Lett. **103**, 047403 (2009).
- [14] For the purpose of numerical calculations, we use either $D(\varepsilon)$ and $v^2(\varepsilon)$ derived from a model of p-like bands or a trial $D(\varepsilon)$, but the origin is not relevant, since only the ε structure is important.
- [15] "See *supplementary material*."
- [16] G. Chiriacò and A. J. Millis, Phys. Rev. B **98**, 205152 (2018).
- [17] J. E. Han, J. Li, C. Aron, and G. Kotliar, Phys. Rev. B **98**, 035145 (2018).
- [18] Alternative choices for transport are possible: for example $\tau_{\text{tr}}(\varepsilon) \propto 1/D(\varepsilon)$ as for impurity scattering, or $v(\varepsilon)\tau_{\text{tr}}(\varepsilon) \sim \text{const}$ as for hard sphere scattering. The results are qualitatively equivalent, with only slight quantitative differences.
- [19] ζ_0 takes into account all the details about the pump fluence, polarization and coupling to the phonon mode. We use reasonable values of ζ_0 , which are roughly estimated by assuming that all the energy of the pump is absorbed by the phonon mode at energy ω_p ; this results in $\zeta_0 \sim 10$ for fluences $\sim 1 \text{ mJ/cm}^2$ and pump penetration lengths $\sim 100 \text{ nm}$.